Inter-Mountain laser communication tests

D. Ruiz, R. Czichy

European Space Agency, ESA/ESTEC, Postbus 2200 AG Noordwijk, The Netherlands

J. Bara, A. Comeron, A. Belmonte

Universidad Politecnica de Cataluna, Departamento de Teoria de Senal y Comunicaciones, ETSI Telecomunicacion, E-08034 Barcelona, Spain

P. Menendez-Valdes, F. Blanco, C. Pedreira

Universidad Politecnica de Madrid, Departamento de Tecnologia Fotonica, ETSI Telecomunicacion, E-28040 Madrid, Spain.

ABSTRACT

As a support activity to the Free-space Optical Communications programme of the European Space Agency, a first evaluation of the Canary Islands (Spain) as optical communication test range has been performed. The low atmospheric attenuation and turbulence induced effects derived from the models have been confirmed by a simple link test.

1. INTRODUCTION

Within ESA's Payload and Spacecraft Development and Experimentation (PSDE) programme, the SILEX project (Semiconductor laser Inter-satellite Link EXperiment) will represent the Agency's first optical communication experiment in space.

The SILEX system is primarily intended as high data-rate optical communications link between a low-earth orbiting satellite and a geostationary relay satellite. A space-to-ground optical link, between the geostationary satellite and an optical ground station, is also planned for the check-out of the spacecraft terminal.

The aim of the Inter-Mountain Laser Communication Experiment was to establish an optical link between two terminals located in far-field conditions. It was initiated to support the PSDE/SILEX project in order to evaluate critical areas of optical communications systems, in particular pointing, acquisition and tracking of the counter terminal and communication through the atmosphere.

The Canary Islands in Spain are an excellent test site to perform this kind of experiment because there are two very high mountains with excellent seeing conditions and a long propagation path over the sea between them.

A basic feasibility study and a first order estimation of the characteristics of the test site have been performed in order to evaluate its potential application as an optical communication test range. A laser-diode based, low-cost experiment was carried out to assess the feasibility of the link and as a first validation of the theoretical analysis.

The following sections explain in more detail the different tasks carried out within this study, namely definition of the characteristics of the test site, analysis of the atmospheric effects in the site and realization of the experiment.

2. GEOGRAPHICAL AND CLIMATIC CHARACTERISTICS OF THE TEST SITE

The Canarian Archipelago (figure 1) lies between 27° 40' N and 29° 25' N latitude, and 13 30' W and 18 10' W longitude, in the Atlantic Ocean, with the most eastward islands at about 100 Km from the Saharian coast.

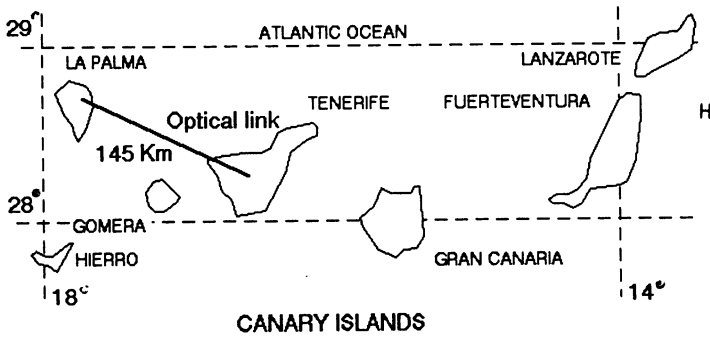

Figure 1. Map of the Canary Islands (Spain)

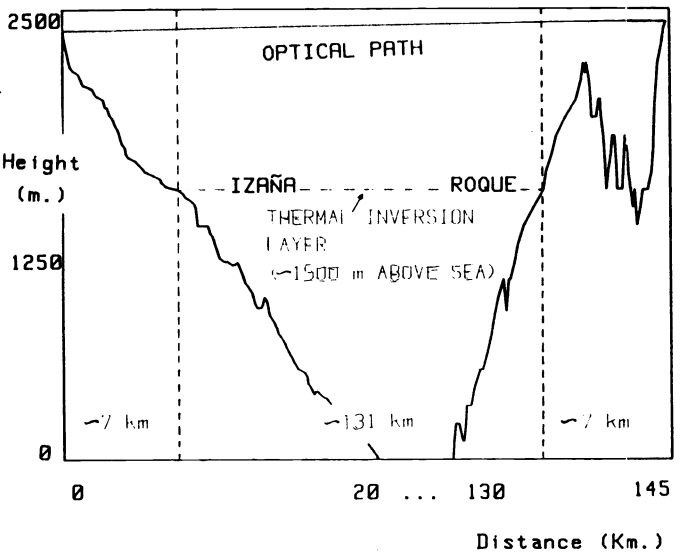

Figure 2. Profile of the ground

The Canary Islands are of volcanic origin. Their mountains (several peaks above 2000 m) have long been identified as excellent sites for astronomical observatories. Their suitability arises not only from their altitude, but also from the stabilizing influence of the sea around the islands. In addition, for most of the year, the islands are under the influence of the trade-winds associated with the Azores' anticyclone. This leads to a situation with a strong stable thermal inversion layer at altitudes ranging from 1000 to 1500 m[1] which results in a shielding effect against humidity and air turbulence in the zone above. Consequently, sites placed higher than the normal altitude range of the thermal inversion layer offer characteristics very much appreciated by astronomers, long observation times and excellent "seeing" (low atmospheric turbulence) conditions.

Two international astrophysical observatories are in operation: Izana on Tenerife and Roque de los Muchachos on La Palma. Both observatories are located at about 2400 m, which is above the thermal inversion layer in normal conditions. They are international consortia with the participation of the Astrophysical Institute of the Canary Islands (IAC) which also manages their activities.

The fact that there is direct line-of-sight between the two observatories, 145 Km apart, and the advantage of the infrastructure, makes it very attractive for optical link experiments.

Based on an analysis of the meteorological data from 1960 to 1987, the availability of an optical link experiment was calculated. A worst case analysis, taking into account all limiting metereological conditions, shows that the optical link between the two islands can be established for a continuous 24-hour period at least 70 % of the days.

3. ATMOSPHERIC EFFECTS

3.1 Refraction effects

Due to the curvature of the Earth, the straight path between two distant points located at the same altitude reaches its minimum height at the mid-point. Since the density of the atmosphere decreases with increasing height, the path becomes inhomogeneous, and atmospheric effects can affect the optical radiation in a different way at any point. In this case, the overall effects must be integrated along the beam. Taking into account the inhomogeneity of the refractive index, the refractivity (N) in the visible and IR region can be expressed as:

$$N = (n-1)x10^6 = C_{dry}(\lambda)(P - e_v)/T + C_{H_2O}(\lambda)\, e_v \qquad (1)$$

n being the refractive index, P and T the atmospheric pressure and temperature, e_v the absolute humidity in units of partial pressure, and C_{dry} and C_{H_2O} are wavelength dependent coefficients accounting for the dispersion of the dry air and the water vapor.

These figures predict a slightly parabolic path with its vertex at about 18.5 m above the mid-point of the straight segment (negligible for a 145 Km path). The emitter and the receiver must be aligned 1.05 mrad above the straight segment between them. The relative variation of the atmospheric density along the path is smaller than 1%, hence the path can be considered homogeneous concerning the calculations of the atmospheric absorption. Figure 2 shows the profile of the ground below the optical path.

3.2 Absorption of radiation and scattering by atmospheric gases

Atmospheric gases present a large number of absorption lines in the IR. For long optical paths, the presence of an absorption line can completely prevent transmission at a given wavelength. Fortunately, the gases present in higher concentrations are either inert (such as Ar) or diatomic molecules (such as N_2 and O_2), which do not absorb in the IR. The main absorbers are water vapor and CO_2. The water content of the atmosphere varies strongly, even during a single day; the other constituents have been considered as uniformly mixed in the proportions indicated in Table 1. The absolute number of molecules of each per volume unit is determined by the air density.

A uniform path where the three atmospheric parameters (pressure, temperature and humidity) are those recorded in Izana since 1960 has been considered (the situation at Roque de los Muchachos should be similar). The absorption of atmospheric gases in the months with the highest and the lowest average air density (January and August respectively) has been estimated. The spectral bands of the different laser sources envisaged for optical free-space communications (790-870 nm, 1.064 nm, 1300 nm, 10.2 micrometers) have been considered[2].

Gases	CO_2	O_3	N_2O	CO	CH_4	NO	NO_2
Concentration	330	0.04	0.28	0.2	1.6	0.002	0.01

Table 1. Relative concentration (ppm by volume) of the absorbing gases taken in the calculations.

Although the first computations have been done at a high resolution (0.045 nm) in the 790 to 870 nm wavelength range[2], the absorption spectrum shown in figure 3 has been averaged in a spectral window of 0.7 nm, due to the fact that laser diodes under modulation may emit multiple longitudinal modes covering a wider spectral region.

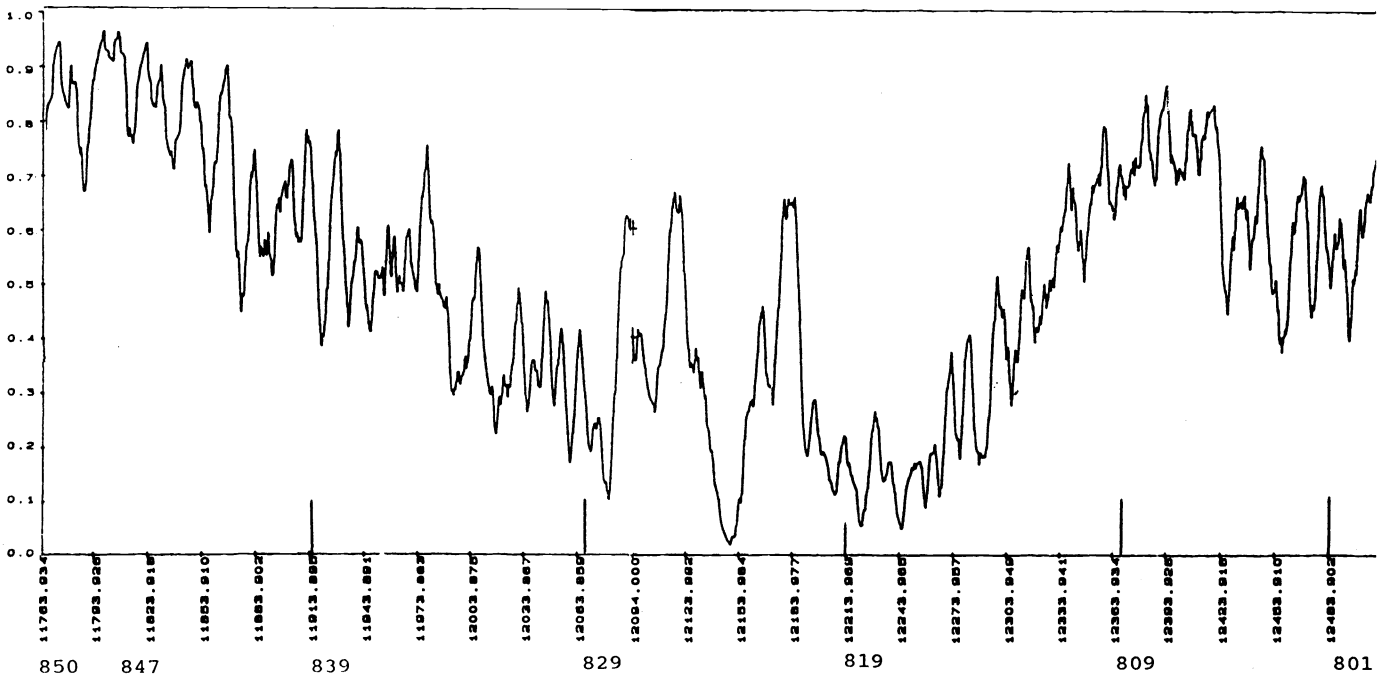

Figure 3. Transmittance of atmospheric gases (100 Km) in the 800-850 nm spectral range vs spatial frequency (inverse of the wavelength). Averaged in a spectral window of 0.7 nm (10 m-1). Atmospheric data (January 1970) are T=276.55 K, P=574.4 Torr, RH = 62%. Some wavelengths to be used in the Silex project (801 nm, 819 nm, 847 nm) are indicated.

Atmospheric gases are transparent to solid state lasers, as Nd:YAG. Hence, they are good candidates for space-to-ground communication links (transmittance around 90 %)[2].

Rayleigh scattering by the atmospheric gases is weak in the IR spectral region, but still noticeable in the 790 to 870 nm range; therefore, it should be considered.

3.3 Aerosols effects

The concentration of particles in the atmosphere at 2400 meters is very small most of the time. Wet maritime hazes do not reach the optical path due to the thermal inversion. Fog is only present when convective air currents lift the clouds along the slopes of the mountains, reaching the altitude of the terminal ends. Calculations based on a semiempiric model[3], have shown that propagation along a short distance (2 Km), under moderate fogs of 1 Km of visual range, attenuates over 40 dB the light emitted at all wavelengths of interest (except at 10.2 micron). Thus, fog must be avoided.

Usually, Sahara dust is the dominant aerosol at the site. Its main component is quartz. Due to its birefringence, an average refractive index of <n>=(2 no + ne)/3 needs to be used as well as the complex refractive index for absorption calculations. A model for the complex refractive index as function of the wavelength for the 790-870 nm region has been derived[2] from several publications[4,5].

Due to abrasion, the dust particles become spherical, so Mie theory of scattering by spherical particles can be applied to quantify the optical attenuation.

Attenuation computed with these refractive indices and the particle distribution functions derived[2] show very low variations in the 790 to 870 nm spectral region. The values are proportional to the dust density. Thus, according to different models the dust attenuation lays between 3.029 x 10-^{4} Km^{-1} and 3.383 x 10^{-4} Km^{-1} per microg/m^3 of dust concentration. The the dispersion between models is around 10%.

No statistics of the dust concentration during the year are available, however our calculations predict concentrations between 7.34 microg/m^3 and 110.0 microg/m^3. These values lead to transmission along the optical path, between more than 68.7 % during clear days, and below 0.71 % under worst case dust invasions.

3.4 Turbulence effects

3.4.1 General Model

Atmospheric turbulence is the random fluctuation of the air velocity around its mean value[6]. When an electromagnetic wave propagates through a turbulent atmosphere its wavefront is distorted in a random way, giving rise to several phenomena[11] (beam spread and wander, intensity scintillation, angle-of-arrival fluctuations) that may affect an atmospheric communications link at optical wavelengths.

These effects will obviously not exist in a space-to-space communications link. Their influence on a terrestrial link should be estimated to assess the extent to which it can be used as a representative test range for spaceborne systems. Although the experiment carried out in the framework of the described project was not intended to perform a full assessment, some quantitative results were obtained.

The amount of the turbulence effects in the electromagnetic wave propagation are mainly determined by the so-called index-of-refraction structure constant (Cn^2), which is a proportionality constant appearing in the expression of the spatial spectrum of the index-of-refraction fluctuations.

To make quantitative predictions, it is necessary to use a model of the dependence of Cn^2 along the optical path. Whilst the dependence of Cn^2 with the height above ground is a fairly involved matter, a very simple model[1,7] was initially used to obtain estimates of the turbulence-induced effects. This model makes the following assumptions:

- Cn^2 is approximately 10^{-15} $m^{-2/3}$ (nighttime), and 10^{-14} $m^{-2/3}$ (daytime), for the optical path sections in which local ground is above the thermal inversion layer.

- Cn^2 is approximately 10^{-17} $m^{-2/3}$ for the optical path sections in which local ground is below the thermal inversion layer.

Figure 2 illustrates the above model taking into account the profile of the ground below the optical path between the two terminal sites. Assuming a 1500 m altitude for the thermal inversion layer the path may be divided in three sections: two approximately 7 Km sections near the terminals (local ground above the inversion layer) and a 131 Km long section that can be considered unaffected by local convection effects. Only spherical wave propagation has been considered due to the relatively large beam divergence used in the experiment

3.4.2 Intensity scintillations

Theoretical expressions for the intensity scintillation at a point of the wavefront exist only for "weak" turbulence. The statistical distribution of the logarithm of the field amplitude (log-amplitude) fluctuations is Gaussian. Its variance (spherical wave) is:

$$s_x^2 = 0.56\, k^{7/6} \int_0^x Cn^2(x')(x'/x)^{5/6}(x-x')^{5/6}\, dx' \qquad (2)$$

with k the wavenumber and x the total path length. This expression ceases giving good predictions for values beyond 0.3. This is the frontier between "weak and strong" turbulence.

With the turbulence model described above, equation (2) gives 7.4 during the day and 1.1 during the night. To estimate the variance that would be encountered in practice, we used the empirical relationship given in figure 4 [8]. In this way, an approximate value of 0.2 for s_x^2 is found both day and night.

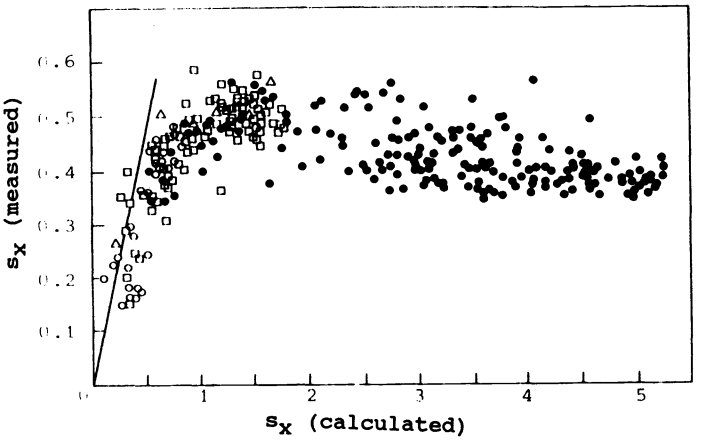

Figure 4. Comparison between the calculated standard deviation of log-amplitude (s_x) using approximations for weak turbulence and measured values.

Assuming a normal log-amplitude, irrespective of the turbulence strength, although some deviations from the Gaussian law do occur, the normalized intensity variance is related to the log-amplitude variance by $s_I^2 = \exp(4s_x^2)-1$.

This would be the variance of the power collected by a point receiver. For a receiver aperture of finite-size, the variance of the collected power will be lower due to the partial incoherence of the intensity fluctuations across the wavefront portion intercepted by the receiving aperture, that results in an averaging effect. The collected power variance can be obtained by multiplying the intensity variance by an averaging factor G(D)[9] that depends on the receiving aperture diameter, D, and on the spatial autocorrelation function of the intensity fluctuations $C_I(p)$ ($C_I(0)=s_I^2$).

As the nighttime value of s_x^2 -after (2)- does not fall too deeply in the saturation region, G(D) was computed using the expressions for the log-amplitude spatial autocorrelation function under weak turbulence[9,10], yielding a 0.87 value for the 17 cm diameter experimental aperture. Daytime conditions give s_x^2 values well inside the saturation region. In this case, the decay of the spatial autocorrelation ($C_I(p)$) seems to occur within distances of the order of the coherence diameter[11]. An estimate of G(D)[12] gives a value 0.12 for a 17 cm diameter aperture.

The above values lead to collected signal log-amplitude variances, assuming a log-normal law for the scintillation of the collected power, of 0.035 (1.63 dB standard deviation) and 0.182 (3.71 dB standard deviation) respectively for day and night conditions.

The spectrum of the intensity fluctuations is determined by the wind velocity component parallel to the optical path, provided that this component is higher than the turbulence-induced fluctuations in air velocity. The order of magnitude of the spectral width is given by the ratio between the transverse wind velocity and the typical correlation distance across the wavefront. When collecting power with a finite-size aperture, the size limiting the spectral width of the collected power fluctuations is rather that of the aperture, if it is larger than the correlation distance[6]. This is the case for a 17 cm diameter aperture and the turbulence model discussed above. Assuming (rather high) transverse wind velocities of the order of 10 m/s, typical spectrum widths of tens of Hz are found.

3.4.3 Angle-of-arrival fluctuations

The mean square value of the angle-of-arrival fluctuations is approximately given by[13]

$$\langle a^2 \rangle = (2.91/D^{1/3}) \int_0^x Cn^2(x')(x'/x)^{5/3}\, dx' \qquad (3)$$

Unlike the scintillation variance, there is no equivalent of the saturation phenomenon for the angle-of-arrival fluctuations, so that equation (3) gives results in good agreement with the observation regardless of the intensity of the turbulence. Assuming the turbulence model above, worst case rms angle-of-arrival fluctuations of 19 microrad are found for daytime conditions, and 6 microrad for nighttime.

The spectrum of the angle-of-arrival fluctuations is also determined by the ratio between transverse wind velocity and the receiving aperture diameter. Its typical bandwidth should be of the same order as that of the fluctuations of the collected power (tens of Hz).

4. EXPERIMENT

To check the predictions of atmospheric attenuation and turbulence effects described in the preceding sections, a test link at 830 nm between the observatories was carried out.

4.1 Location and equipment

The transmitter was installed on the 9th floor, north face of the Vacuum Telescope Tower, (Izana Observatory), the receiver was located in a tent installed in a flat piece of ground in front of the Jacobus Kapteyn Telescope (Roque de los Muchachos Observatory).

The scheme of the link is the following: The laser, modulated by a square wave of 10 kHz, is collimated by a transmitting telescope, and is received by another telescope with a photodiode in its focal plane. Its output is amplified, filtered and properly detected, prior to its final measurement. The following components were used:

- Transmitting laser (GALA-083-25-1) :

Wavelength (25 C), full CW power: 832 nm
Linewidth (as above): 0.067 nm
Maximum CW power: 40 mW
Modulation depth: 80%

- Transmitting telescope.

A 10 cm diameter refractive telescope was used to accomplish beam divergence control and visual pointing. Two gimballed mirrors (5 cm and 15 cm) provided fine and coarse pointing capabilities. The equipment was installed on a 80 cm x 120 cm optical table.

Telescope transmission: 25% (-6 dB)
Divergence control: adjustable by a factor >10.
Nominal divergence, $2\Theta_x$: 0.86 mrad
$2\Theta_y$: 0.35 mrad

- Receiving Telescope

A 7 inch Questar telescope was used with the following characteristics:

Focal length: 280 cm
Aperture diameter: 17.5 cm
Obscuration diameter: 6.25 cm
Transmittance at 830 nm: 65%

Several color and interference filters were used to reduce the background noise. The transmission was of the order of 80 %, depending on the laser wavelength drifts.

- Photodetector

The photodiode used was a 10x10 mm^2 EGG HUV-4000B. Its characteristics are as follows:

Bandwidth: 0 - 14 kHz
DC responsivity: 5.3 mV/nW
AC responsivity (output amplitude -sinusoidal- vs square wave optical input): 3.0 mV/nW
Noise power density (10 kHz): 8.8E-6 V/ Hz

- Position sensitive photodetector (PSD)

A SiTek position sensitive detector with 10x10 mm^2 active area was also used to monitor angle of arrival fluctuations. By combining its output signals, three basic outputs are obtained: a DC voltage proportional to the amplitude of the input optical wave, two DC voltages proportional to the X and Y positions of the light spot in the active surface.

- Detector electronics

Two different instruments were used to measure the 10 kHz voltage signal: A precision full-wave rectifier with suitable filtering, and a tuned amplifier followed by a detector (Hewlett-Packard 415E) with 60 dB gain and adjustable bandwidth (320-2800 Hz) (figure 5).

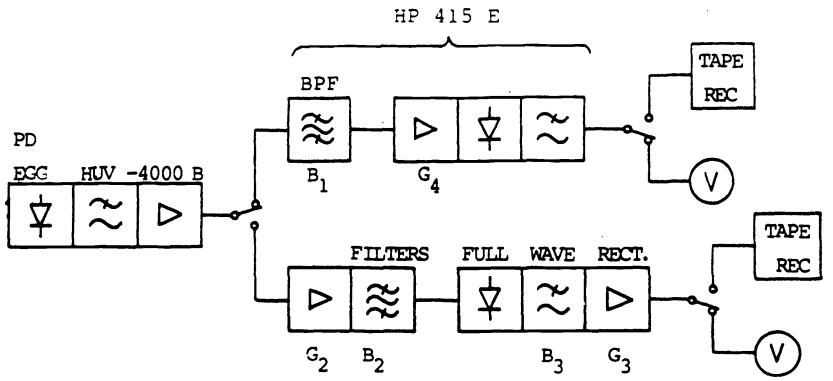

Figure 5. Receiver configuration

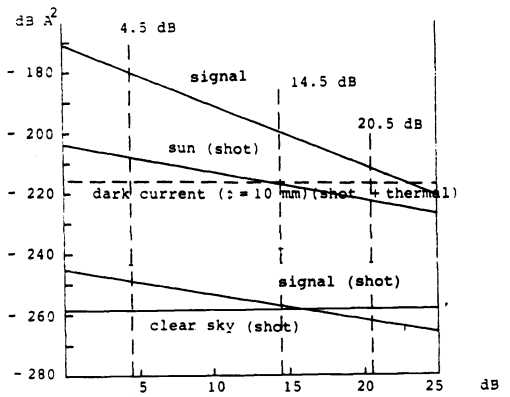

Figure 6. Link budget. Current values at the photodiode output.

4.2 Link budget

With the above data for the experimental equipment, the link budget can be derived.

- Free space attenuation

For far field conditions, we have the following intensity at the beam axis:

$$[u]^2 = 2Po/(z^2\Theta_x\Theta_y) \qquad (4)$$

Θ_x, Θ_y are half the values quoted before, and Po is the total power out of the collimating telescope. The considered pointing loss is of the order of 1 dB.

- Gases/aerosols attenuation

In view of the theoretical analysis, the following figures are taken for the 145 Km path.

Clear air: -4.5 dB (50 % transmission in 100 Km)
Low visibility: -14.5 dB (10 % transmission in 100 Km)

Higher values of attenuation could be obtained in the events of fogs or Saharian dust.

- Background radiation

Only a bright sky is considered, since with the optical filters, weaker background sources (moon, stars, etc.) turn out to be negligible. The event of having the sun fully in the field of view (rather exceptional), is also considered as a extreme source of background radiation. A 1 mm diameter diaphragm is assumed in front of the photodiode.

Considering a sun apparent diameter of 32', it turns out that the sun irradiance at 830 nm outside the atmosphere is 1.52 E7 W/m2/um/sr. Concerning the clear sky radiation, for 0^{o} elevation angle, a worst case value of 50 W/m2/um/sr has been considered, . This radiation would be attenuated by aerosols., but clear atmosphere absorption is included in the data above.

- Bandwidth

According to the turbulence analysis the spectrum of signal will not have significant components beyond 100 Hz. Thus, a predetection filter maximum bandwidth of 300 Hz is taken.

- Signal and noise budgets

Figure 6. shows signal and noise currents as a function of atmospheric attenuation. With the 10x10 mm^2 EGG detector, the shot noise levels due to the signal and the clear sky background induced currents are negligible. Even with the sun in the field of view, the S/N for low atmospheric attenuation (4.5 dB) is around 25 dB.

4.3 Results

The total observation time was 15 hours, 9 during the day and 6 during the night. Within this time, 90 min of data were recorded with a tape recorder. Observations can be grouped in blocks corresponding to periods of 1-2 hours during which transmission parameters remained fairly constant (+- 0.5 dB). Results obtained were as follows:

- Attenuation

A fairly stable, minimum attenuation value of ca. 3.5 dB was measured during at least half the observation time. The maximum measured attenuation did not exceed 12 dB.

- Power scintillation

A statistical analysis of the data recorded in Roque de los Muchachos was performed by carrying out a Kolmogorov-Smirnov test of the samples against a Gaussian distribution.

Measured log-amplitude variance (nighttime, minimum attenuation) was 0.25 (4.35 dB standard deviation), while computed log-amplitude variance is 0.18 (3.71 dB standard deviation). Figure 7. shows the sample histogram of the received amplitude. Agreement with the predicted Gaussian distribution can be taken as a validation of the measurement. The measured figures suggest a situation near the saturation limit, with long correlation radius that make aperture averaging of little importance.

- Spectrum analysis

The measured spectral width of the scintillation at -20 dB is somewhat more than 50 Hz. Although the transverse component of wind velocity along the path was not measured during the experiment, the range of the measured spectral widths agrees with the predictions.

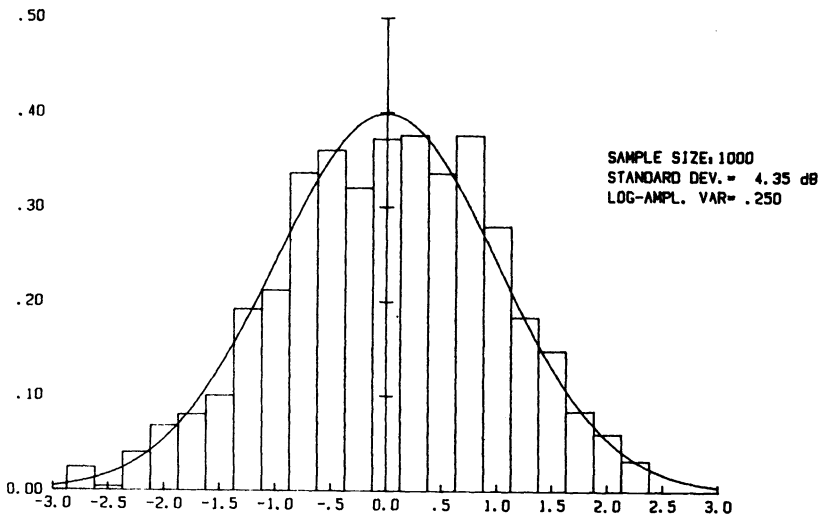

Figure 7. Sample histogram of the received amplitude. Gaussian approximation.

- Angle of arrival fluctuations

They were measured with the SiTek PSD. The X-Y position accuracy was greatly degraded when the optical power levels received (between -54 and -48 dBm) were in the lower end of the quoted range. A selection of the values recorded during the periods of strong received signal, due to scintillation, produced the following values:

Daytime standard deviation.	Measured: 19.8 microrad Computed: 19 microrad
Nighttime standard deviation.	Measured: 7.0 microrad Computed: 6 microrad

Since the statistical analysis has been carried out with a low number of valid points, these results should be taken with some care. Also, the agreement between computed and measured values should not be considered especially significant, given the simple model used for the computation of turbulence induced effects.

5. CONCLUSION

The study of the geographical and climatic characteristics of the test site and the theoretical analysis of its atmospheric conditions have shown that the Canary Islands are a proper site to perform terrestrial experiments of free-space optical communication systems.

The low atmospheric attenuation and turbulence induced effects derived from the models have been confirmed by the simple link test carried out. In particular, the low attenuation over the 143.5 Km horizontal path, demonstrates clearly the feasibility of a space-to-ground optical link and consequently installation of optical ground station.

This study was considered as a feasibility study. More detailed experimental work is necessary to provide additional data concerning spatial/spectral atmospheric characteristics and to establish a complete and verified model of the space-to-ground and free-space optical links by means of terrestrial experimentation.

6. ACKNOWLEDGMENTS

We wish to express our thanks to our colleague V. Freudenthaler (ESA/ESTEC) for his efficient work throughout this study; to F. Sanchez, P. Alvarez, E. Ballesteros, F.J. Fuentes (Astrophysical Institute of the Canary Islands) and E. Schroter, W. Mattig (Kiepenheuer-Institut) for the excellent support during the experiment activities and to B. Moreau, R. Jalin (ONERA-France) for their contribution to the study.

The results presented in this article have been obtained under the ESA Contract No: 8131/88/NL/DG. "Assessment of atmospheric losses on an optical link budget"[2].

7. REFERENCES

1. F.J. Fuentes, C. Munoz-Tunon, "Climatologia y turbulencia atmosferica en los observatorios canarios", IAC Internal Report.
2. "Assessment of atmospheric losses on an optical link budget" ESA Contract No 8131/88/NL/DG. Universidad Politecnica de Cataluna, Barcelona, Spain
3. P. Menendez-Valdes, F. Blanco, Proc. of the VII Reunion de la Comision B (Campos y Ondas), URSI, Spanish Committee; Cuenca (Spain), Sept. 1988.
4. P. Murdin, RGO/La Palma Technical Note No 31, April 1986.
5. E.M. Patterson, D.A. Gillette, B.H. Stockton, J. Geophys. Res. 82, 3153 (1977).
6. V.I. Tatarski. "Wave propagation in a turbulent medium", McGraw-Hill, 1961.
7. B. Moreau, R. Jalin (ONERA-France), IAC Internal Report.
8. J.W. Strohbehn, "Line-of-Sight Wave Propagation Through the Turbulent Atmosphere", Proc. of the IEEE,Vol. 56, No. 8, pp. 1301-1318, Aug. 1968.
9. D.L. Fried, "Aperture Averaging of Scintillation", Jour. Opt. Soc. Am., Vol. 57, No. 2, pp. 169-175, Feb. 1967.
10. R.F. Lutomirski, H.T. Yura, "Aperture-Averaging Factor of a Fluctuating Light Signal", Jour. Opt. Soc. Am., Vol. 59, No. 9, pp. 1247-1248, Sept. 1969.
11. R.L. Fante, "Electromagnetic Beam Propagation in Turbulent Media", Proc. IEEE, Vol. 63, No. 12, pp. 1669-1692, Dec. 1975.
12. G.R. Ochs, R.R. Bergman, J.R. Snyder, "Laser beam Scintillation over Horizontal Paths from 5.5 to 145 Km", Jour. Opt. Soc. Am., Vol. 59, No. 2, pp. 231-234, Feb. 1969.
13. R.E. Hufnagel, "Propagation through atmospheric turbulence", in The Infrared Handbook (Ed. by William L. Wolfe and George J. Zissis), chap. 6. Office of Naval Research, Dept. of the Navy, 1978.